J. Mater. Environ. Sci. 7 (8) (2016) 2806-2819
ISSN : 2028-2508
CODEN: JMESCN

Inhibitive Properties and Quantum Chemical Studies of 1,4-Benzothiazine Derivatives on Mild Steel Corrosion in Acidic Medium

M. Ellouz[1], N. K. Sebbar[1], H. Elmsellem[2*], H. Steli[5], I. Fichtali[3], M. M. Mohamed Abdelahi[1], K. Al Mamari[1,4], E. M. Essassi[1], I. Abdel-Rahaman[6]

[1]*Laboratoire de Chimie Organique Hétérocyclique, URAC 21, Pôle de Compétences Pharmacochimie, Mohammed V University in Rabat, Faculté des Sciences, Av. Ibn Battouta, BP 1014 Rabat, Morocco.*

[2] *Laboratoire de chimie analytique appliquée, matériaux et environnement (LC2AME), Faculté des Sciences, Université Mohammed Premier B.P. 717, 60000 Oujda, Morocco*

[3]*Laboratoire de Chimie Organique Appliquee, Université Sidi Mohamed Ben Abdallah, Faculté des Sciences et Techniques, Route d'Immouzzer, BP 2202 Fes, Morocco.*

[4]*Department of Chemistry - Faculty of Education University of Hodiedah – Yemen.*

[5]*Laboratoire mécanique & énergétique, Faculté des Sciences, Université Mohammed Premier, Oujda, Maroc*

[6]*Department of Chemistry, College of Sciences, University of Sharjah, Sharjah, PO Box: 27272, UAE.*

Received 21 May 2015; Revised 30 June 2016; Accepted 4 July 2016.
**Corresponding author. E-mail: h.elmsellem@yahoo.fr; Tél : +212670923431*

Abstract

4-Benzyl-2-substituted-[1,4]-benzothiazin-3-one derivatives (P3 and P4) , were synthesized from 2-substituted-[1,4]-benzothiazin-3-one . The structures of all newly synthesized compounds were elucidated by elemental analysis, 1H-NMR and 13C-NMR. Adsorption of compounds (P3 and P4) on mild steel surface in 1 M HCl solution and its corrosion inhibition properties has been studied by a series of techniques, such as polarization, electrochemical impedance spectroscopy (EIS), weight loss and quantum chemical calculation methods. The experimental results suggest that these compounds are an efficient corrosion inhibitors and the inhibition efficiency increases with the increase in inhibitors concentration. Adsorption of these compounds on mild steel surface obeys Langmuir's isotherm. Correlation between quantum chemical calculations and inhibition efficiency of the investigated compounds are discussed using the Density Functional Theory method (DFT).

Keywords: Mild steel, 1,4-Benzothiazine, EIS, Corrosion, Weight loss, Electrochemical, DFT.

1. Introduction

The study of corrosion inhibition is a very active field of research. Several classes of organic compounds are widely used as corrosion inhibitors for metals in acid environments.[1–3]. Experimental means are useful to explain the inhibition mechanism but they are often expensive and time-consuming. Ongoing hardware and software advances have opened the door for the powerful use of theoretical chemistry in corrosion inhibition research. Several quantum chemical methods and molecular modeling techniques have been performed to correlate the inhibition efficiency of the inhibitors with their molecular properties.[4–6]. Using theoretical parameters helps to characterize the molecular structure of the inhibitors and to propose their interacting mechanism with surfaces [7].

[1,4]-Benzothiazine derivatives, has largely been studied in various fields of chemistry, including chemical and pharmaceutical industries. These compounds have more active sites, which confer them a high reactivity, making them an excellent heterocyclic precursor in the synthesis of new heterocyclic systems possessing an

interesting biological activities such as anti-inflammatory [8], analgesic [9], anti-microbial,[10] and anti-oxidant agents [11]. They have also been reported as synthetic intermediates for other drugs,[12] as stabilizers in rubber vulcanization [13], and corrosion inhibitors [14]. The present study aimed to test new compounds namely [4-benzyl-2-substituted-[1,4]-benzothiazin-3-one]: (P3 and P4) on the corrosion of mild steel in 1 M hydrochloric acid solution. In this work, we are interested in the synthesis of the title compounds for biological activities, by realizing the alkylation reaction with benzyl chloride in DMF, the residue was extracted with water, the organic compound was chromatographed on a column of silica to give compounds (P3, P4) (**Scheme 1**).

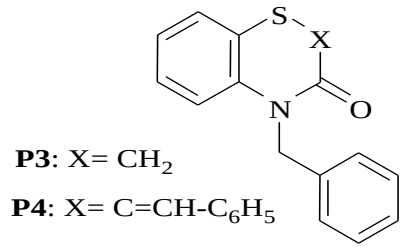

Scheme 1: 4-benzyl-2-substituted-[1,4]-benzothiazin-3-one (P3 and P4)

2. Experimental

2.1. Synthesis of inhibitors

To a solution of 2-substituted-[1,4]-benzothiazin-3-one (2 mmol), potassium carbonate (0.55 g, 4 mmol) and tetra *n*-butyl ammonium bromide (TBAB) (0.064 g, 0.2 mmol) in DMF, (15 ml) was added benzyl chloride (0.46 ml, 4 mmol). Stirring was continued at room temperature for 12 h. The mixture was filtered and the solvent removed. The residue was extracted with water. The organic compound was chromatographed on a column of silica gel with ethyl acetate-hexane (9/1) as eluent (**Scheme 2**):

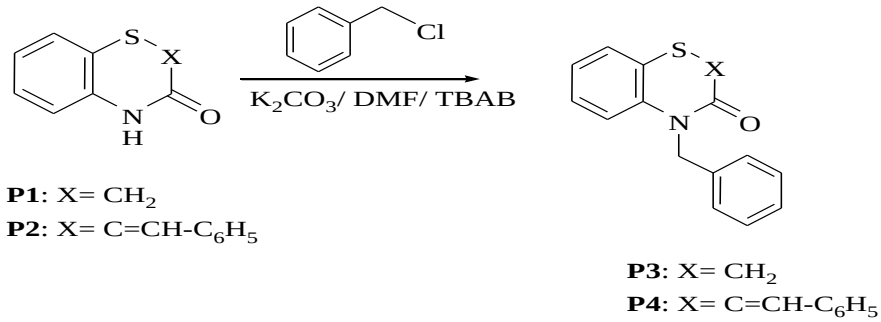

Scheme 2: Synthesis of 4-benzyl-2-substituted-[1,4]-benzothiazin-3-ones (**P3 and P4**).

The analytical and spectroscopic data are conforming to the structure of compounds formed:
(P3): Yield: 75%**; MP =** 365-367 **K; NMR^{1}H (DMSO-d6) δ ppm:** 6.95-7.39 (m, 9H_{arom}); 5.21 (s, 2H, NCH_2); 3.63 (s, 2H, SCH_2). **NMR^{13}C (DMSO-d6) δ ppm**: 165.7 (C=O); 139.5, 137.4, 123.7 (C_q); 129.0, 128.5, 127.6, 127.4, 126.7, 123.8, 118.7 (CH_{arom}); 47.1 (NCH_2); 30.7 (SCH_2).
(P4): Yield: 76%; MP = brown oil**; NMR^{1}H (DMSO-d6) δ ppm:** 7.89 (s, 1H, =CH-C_6H_5); 6.98-7.67 (m, 14H_{arom}); 5.35 (m, 2H, NCH_2). **NMR^{13}C (DMSO-d6) δ ppm:** 161.3 (C=O); 137.1, 136.4, 134.6, 120.6, 118.2 (C_q); 134.8 (CH_2); 130.5, 129.6, 129.2, 129.1, 127.8, 127.5, 126.7, 126.6, 124.2, 118.4 (CH_{arom}); 48.3 (CH_2).

2.2. Quantum chemical calculations

Quantum chemical calculations are used to correlate experimental data for inhibitors obtained from different techniques (viz., electrochemical and weight loss) and their structural and electronic properties. According to Koop man's theorem [15], E_{HOMO} and E_{LUMO} of the inhibitor molecule are related to the ionization potential (I) and the electron affinity (A), respectively. The ionization potential and the electron affinity are defined as I =

$-E_{HOMO}$ and $A = -E_{LUMO}$, respectively. Then absolute electronegativity (χ) and global hardness (η) of the inhibitor molecule are approximated as follows [16]:

$$\chi = \frac{I+A}{2}\ ,\ \ \chi = -\frac{1}{2}(E_{HOMO} + E_{LUMO}) \textbf{ (1)}$$
$$\eta = \frac{I-A}{2}\ ,\ \ \eta = -\frac{1}{2}(E_{HOMO} - E_{LUMO}) \textbf{ (2)}$$

Where $I = -E_{HOMO}$ and $A = -E_{LUMO}$ are the ionization potential and electron affinity respectively.
The fraction of transferred electrons ΔN was calculated according to Pearson theory [17]. This parameter evaluates the electronic flow in a reaction of two systems with different electronegativities, in particular case; a metallic surface (Fe) and an inhibitor molecule. ΔN is given as follows:

$$\Delta N = \frac{\chi_{Fe} - \chi_{inh}}{2(\eta_{Fe} + \eta_{inh})} \textbf{ (3)}$$

Where χFe and χinh denote the absolute electronegativity of an iron atom (Fe) and the inhibitor molecule, respectively; ηFe and ηinh denote the absolute hardness of Fe atom and the inhibitor molecule, respectively. In order to apply the eq. 3 in the present study, a theoretical value for the electronegativity of bulk iron was used χFe = 7 eV and a global hardness of ηFe = 0, by assuming that for a metallic bulk I = A because they are softer than the neutral metallic atoms [17].
The electrophilicity has been introduced by Sastri et al. [18], is a descriptor of reactivity that allows a quantitative classification of the global electrophilic nature of a compound within a relative scale. They have proposed the ω as a measure of energy lowering owing to maximal electron flow between donor and acceptor and ω is defined as follows.

$$\omega = \frac{\chi^2}{2\eta} \textbf{ (4)}$$

The Softness σ is defined as the inverse of the η [19]:

$$\sigma = \frac{1}{\eta} \textbf{ (5)}$$

Using left and right derivatives with respect to the number of electrons, electrophilic and nucleophilic Fukui functions for a site k in a molecule can be defined [20].

$$f_k^+ = P_k(N+1) - P_k(N) \quad for\ nucleophilic\ attack \textbf{ (6)}$$
$$f_k^- = P_k(N) - P_k(N-1) \quad for\ electrphilic\ attack \textbf{ (7)}$$
$$f_k^+ = [P_k(N+1) - P_k(N-1)]/2 \quad for\ radical\ attack \textbf{ (8)}$$

where, $P_k(N)$, $P_k(N+1)$ and $P_k(N-1)$ are the natural populations for the atom k in the neutral, anionic and cationic species respectively.

3. Results and discussion

3.1. Weight loss measurements

In general, the efficiency of an organic substance as an inhibitor for metallic corrosion depends on structure and the concentration of inhibitor [21]. In order to study the action of these parameters on mild steel corrosion, some experiments were carried out. The corrosion rate *w* (mg cm^{-2} h^{-1}), the surface coverage (θ) and the values of inhibition efficiency E_w (%) obtained from weight loss measurements of mild steel after 6 h immersion in molar HCl solutions at various concentrations of P3 and P4 at 308K are shown in Table 1.

$$\rho = \frac{\Delta W}{At} \textbf{ (9)}$$

Where ΔW is the average weight loss of the mild steel specimens, A is the total area of mild steel specimen and t is the immersion time. The percentage inhibition efficiency (E_w%) was calculated using the relationship:

$$Ew\ (\%) = \frac{W0 - Wi}{W0} \text{ x } 100 \qquad \textbf{(10)}$$

Where w_0 and w_i are the weight loss values in the absence and presence of inhibitor.

Table 1: Corrosion parameters obtained from weight loss measurements of mild steel after 6h immersions in 1 M HCl solution with and without addition of various concentrations of benzothiazine derivatives P3 and P4 at 308k.

Inhibitor	**Concentration** (M)	***v*** ($mg.cm^{-2}\,h^{-1}$)	$\mathbf{E_w}$ (%)	**θ**
1M HCl	-	0.82	---	---
P3	$\mathbf{10^{-6}}$	0.43	48	0.48
	$\mathbf{10^{-5}}$	0.34	59	0.59
	$\mathbf{10^{-4}}$	0.21	74	0.74
	$\mathbf{10^{-3}}$	0.16	80	**0.80**
P4	$\mathbf{10^{-6}}$	0.31	62	0.62
	$\mathbf{10^{-5}}$	0.22	73	0.73
	$\mathbf{10^{-4}}$	0.19	77	0.77
	$\mathbf{10^{-3}}$	0.11	87	**0.87**

Data in Table 1 reveals that the addition of benzothiazine derivatives decreases the corrosion rate of mild steel, while inhibition efficiency (E*w*) and surface coverage (θ) increase with increasing inhibitors concentration at 308k,

At a concentration of 10^{-3}M the benzothiazine derivatives (P3; P4) exhibits maximum inhibition efficiency (80% of P3 and 87% of P4 in 1 M HCl), which represents efficient inhibitive ability. This can be due to the inhibitor molecules act by adsorption on the metal surface [22].

3.2. Polarization curves measurements

Figure 1 shows anodic and cathodic polarization plots recorded on mild steel electrode in 1 M HCl in absence and presence of different concentrations of P3 and P4. Electrochemical corrosion parameters, such as corrosion potential E_{corr}(mV/SCE), cathodic and anodic Tafel slopes βc (mV/dec), the corrosion current density I_{corr} (µA cm^{-2}) and inhibition efficiency Ep (%) are given in Table 2. The percentage of inhibition efficiency Ep was calculated following this equation [23]:

$$Ep\% = \frac{\text{icor (0)} - \text{icor (inh)}}{\text{icor (0)}} \text{x } 100 \qquad \textbf{(11)}$$

Where $i_{corr}(0)$ and $i_{corr}(inh)$ represent corrosion current density values without and with the inhibitor, respectively.

It is clear from Figures 1 and 2 that the presence of benzothiazine derivatives (P3 and P4) decreases cathodic and anodic slopes with the increasing inhibitor concentration in both acids. As it can be seen from Table 2, in both solutions when the concentration of inhibitors increases the inhibition efficiencies increase, while corrosion current densities decrease. From Table 2 also can find that the corrosion potentials of inhibitors benzothiazine derivatives (P3 and P4) in the positive direction in HCl solution and shift in the negative direction in HCl solution.

These results indicate that (P3 and P4) are mixed type inhibitor (predominant cathodic effectiveness) acting on both the hydrogen evolution reaction and metal dissolution. The cathodic current–potential curves (Figures 1 and 2) give rise to parallel lines indicating that the addition of P3 and P4 to the HCl solutions does not modify the hydrogen evolution mechanism and the reduction of H^+ ions at the mild steel surface which occurs mainly through a charge transfer mechanism.

ISSN : 2028-2508
CODEN: JMESCN

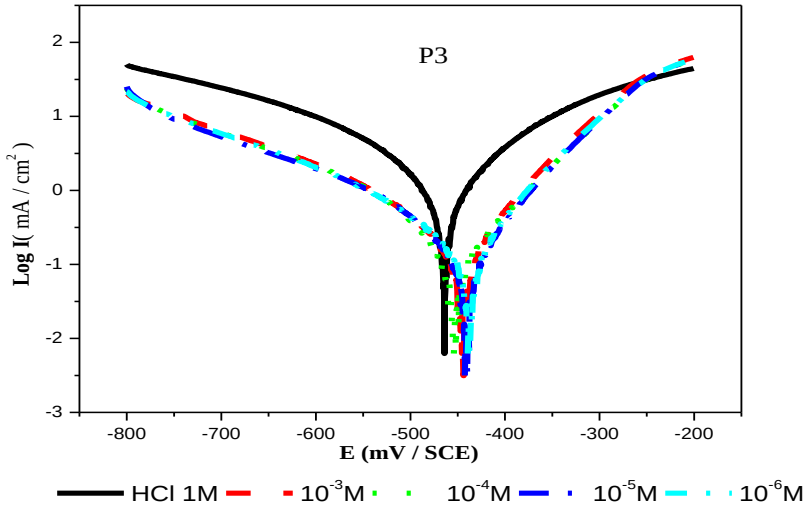

Figure 1: Potentiodynamic polarization curves for mild steel in 1 M HCl without and with different concentrations of P3 at 308 K.

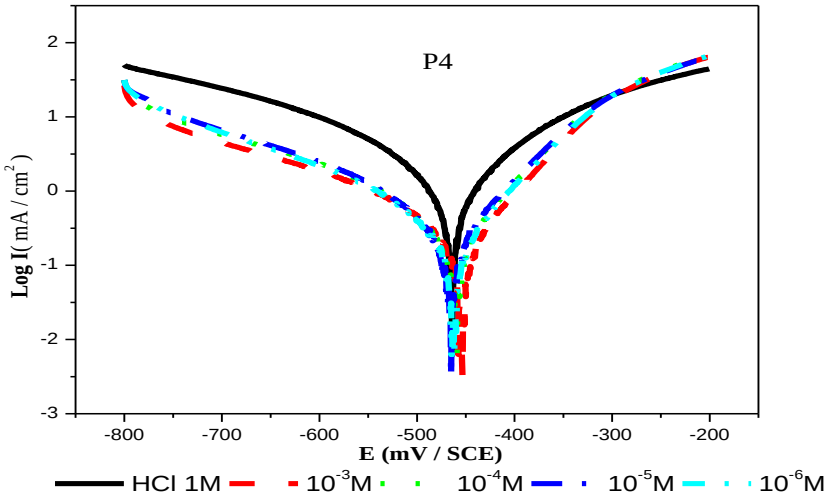

Figure 2: Potentiodynamic polarization curves for mild steel in 1 M HCl without and with different concentrations of P4 at 308 K.

Table 2. Potentiodynamic polarization parameters for the corrosion of mild steel in 1 M HCl solution containing different concentrations of inhibitors P3 and P4 at 308K.

Inhibitor	**Concentration** (M)	**-E_{corr}** (mV/SCE)	**I_{corr}** ($\mu A/cm^2$)	**-βc** (mV dec^{-1})	**E_p** (%)
1M HCl	**-**	464	1386	184	--
P3	**10^{-6}**	457	475	154	66
	10^{-5}	442	380	147	73
	10^{-4}	444	250	153	82
	10^{-3}	455	127	125	**91**
P4	**10^{-6}**	460	409	161	70
	10^{-5}	461	348	139	75
	10^{-4}	463	246	153	82
	10^{-3}	459	109	165	**92**

The inhibitor molecules are first adsorbed onto mild steel surface and blocking the available reaction sites. In this way, the surface area available for H^+ ions decreases while the actual reaction mechanism remains unaffected [24]. These results are in good agreement with the results obtained from weight loss measurements. That is, the inhibition efficiency increases by increasing of inhibitors benzothiazine derivatives (P3 and P4) concentration. This may be due to the increase in (P3 and P4) concentration leads to increasing the surface coverage of the inhibitors and hence increase the adsorption on the mild steel surface.

3.3. Electrochemical impedance spectroscopy measurements

In order to better define the effect of our additive and concentration on the corrosion process, Nyquist plots of mild steel in uninhibited and inhibited acidic solution 1M HCl containing various concentrations of benzothiazine derivatives (P3 and P4) are shown in Figures 3 and 4.

The existence of a single semicircle shows a single charge transfer process during dissolution which is unaffected by the presence of inhibitors molecules. Deviations from perfect circular shape are often referred to the frequency dispersion of interfacial impedance which arises due to surface roughness, impurities, dislocations, grain boundaries, adsorption of inhibitors, and formation of porous layers and inhomogenates of the electrode surface [25, 26].

Transfer resistance Rt (Ω cm^2), double layer capacitance C_{dl} (μF cm^{-2}) and the inhibitor efficiency values E (%) are given in Table 3. Double layer capacitance values were obtained at maximum frequency (f_{max}) at which the imaginary component of the Nyquist plot is maximum and calculated using the following equation:

$$C_{dl} = \frac{1}{2\pi . f_{\max} R_{ct}} \quad \textbf{(12)}$$

The inhibition efficiency E_{Rct}(%) was calculated using the polarization resistance as follows:

$$E_{Rct}\% = \frac{R_{ct\,(inh\,)} - R_{ct\,(0)}}{R_{ct\,(inh\,)}} \text{x } 100 \quad \textbf{(13)}$$

Where $R_{ct(0)}$ and $R_{ct(inh)}$ are the charge transfer resistance values in the absence and presence of inhibitor, respectively.

As seen from Figures 3 and 4 the diameter of the semicircle increases after the addition of P3 and P4 to the aggressive solution. This increase more and more pronounced with increasing inhibitors concentration. It is evident from these results that benzothiazine derivatives (P3 and P4) inhibits the corrosion of mild steel in 1 M HCl at all the concentrations used, and the inhibition efficiency (E_{Rct}) increases continuously with increasing concentration at 308K. EIS results (Table 3) show that the R_t values increase and the C_{dl} values decrease with increasing the inhibitors concentration.

Table 3: EIS parameters for the corrosion of mild steel in 1 M HCl solution containing different concentrations of P3 and P4 at 308 K.

Inhibitor	**Concentration** (M)	**R_{ct}** (Ω .cm^2)	**Rs** (Ω.cm^2)	**CPE** ($\mu\Omega^{-1}S^n$ cm-^{2})	**n**	**f_{max} (Hz)**	**C_{dl} (µF)**	**E_{Rct} (%)**
1M HCl	--	14.50	1.93	393	0.88	11	200	--
P3	**10^{-6}**	78	1.99	184	0.79	20	64	81
	10^{-5}	97	3.24	244	0.75	16	61	85
	10^{-4}	117	1.95	150	0.80	14	55	88
	10^{-3}	133	2.32	122	0.82	12	51	**89**
P4	**10^{-6}**	90	2.15	156	0.81	18	61	84
	10^{-5}	124	2.34	178	0.76	13	51	88
	10^{-4}	126	2.36	136	0.80	13	46	88
	10^{-3}	295	4.32	207	0.64	5	35	**95**

The increase in R_t value can be attributed to the formation of protective film on the metal/solution interface. In fact, the decrease in C_{dl} values can result from a decrease in local dielectric constant and/or an increase in the thickness of the electrical double layer. It can be assumed that the decrease of C_{dl} values is caused by the gradual replacement of water molecules by adsorption of inhibitor molecules on the mild steel surface [27]. The increase in values of Rct and the decrease in values of C_{dI} with increasing the concentration also indicate that the benzothiazine derivatives acts as primary interface inhibitors and the charge transfer controls the corrosion of steel under the open circuit conditions.

The semicircle actually corresponds to one time constant process as even resulted in the Bode phase plots (Figures 5 and 6). In fact, the adsorption mechanism, which involves more than one time constant, takes into account also interaction phenomena between the inhibitors molecules behind the inhibitors– metal surface adsorption reaction, and this, seemed to not happen in our case. The impedance study also gave the same efficiency trend as found in Tafel polarization and weight loss methods.

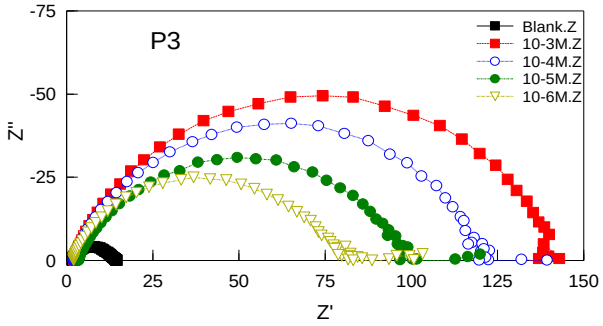

Figure 3: Nyquist diagram for mild steel in 1 M HCl solution in the absence and presence of different concentrations of **P3**.

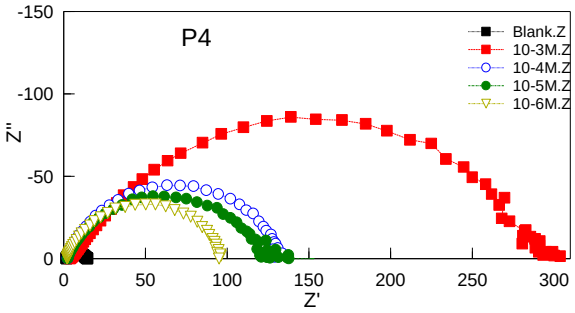

Figure 4: Nyquist diagram for mild steel in 1 M HCl solution in the absence and presence of different concentrations of **P4**.

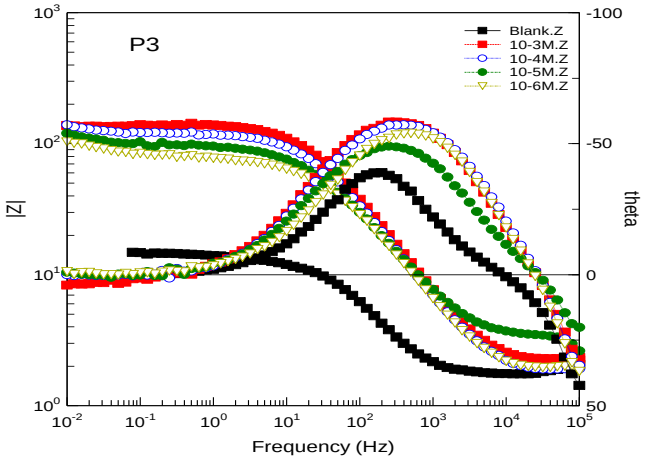

Figure 5: Bode and Phase angle plots of mild steel in 1 M HCl in the absence and presence of different concentrations of **(P3)** at 308K.

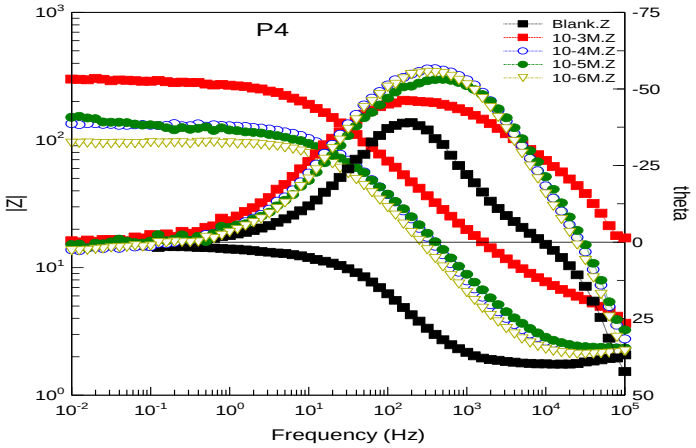

Figure 6: Bode and Phase angle plots of mild steel in 1 M HCl in the absence and presence of different concentrations of **(P4)** at 308K.

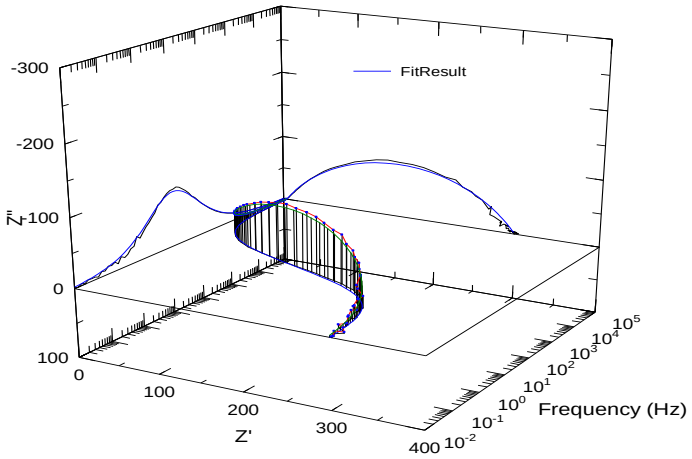

Figure 7: EIS Nyquist and Bode diagrams 3D for mild steel/1 M HCl + 10^{-3} M of **P4** interface: (------) experimental; (------) fitted data.

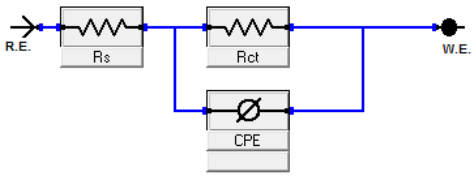

Figure 8: Equivalent circuit model used to fit the impedance spectra.

3.4. Adsorption isotherm and thermodynamic consideration

The adsorption isotherms are considered to describe the interactions of the inhibitor molecule with the active sites on the metal surface [28], several adsorption isotherms were attempted to fit θ values to standard isotherms including that of Fumkin, Temkin, Freundlich , Floy-Huggins and Langmuir isotherm [29]. All these models were compared according to two statistical parameters, i.e. correlation coefficient R^2 and Root Mean Square Error (RMSE), they were used as the primary criteria to select the best isotherm. The RMSE gives the deviation between the predicted and experimental values and it is preferred tending to zero. The degree of surface coverage (θ) values have been evaluated from the Weight loss measurements as a function of the concentration of the inhibitor (C) was tested graphically by fitting it to various isotherms to find the best fit which describes this study. Langmuir adsorption isotherm was found to give the best description for benzothiazine derivatives (P3 and P4) on mild steel. This isotherm can be represented as [30]:

$$\frac{\theta}{1-\theta} = C_{inh}.K_{ads} \qquad \textbf{(14)}$$

K_{ads} is the adsorptive equilibrium constant representing the interaction of the additive with the metal surface. The linear relationships of C /θ versus C, depicted in Figure 9 suggest that the adsorption of P3 and P4 on the mild steel in both the acids obeys Langmuir adsorption isotherm. This model assumes that the solid surface contains a fixed number of adsorption sites and each site holds one adsorbed species [31]. The constant K_{ads} is related to the standard free energy of adsorption $\Delta G°_{ads}$ (kJ mol^{-1}) by the equation:

$$\Delta G°_{ads} = - RT\, Ln\, (K_{ads}\, 55.5) \qquad \textbf{(15)}$$

Where R is universal gas constant; 8.3144 J. K^{-1} mol^{-1}, T is the temperature in K. The value of 55.5 is the concentration of water in solution expressed in moles per liter. The high values of K_{ads} and negative values of (Table 4) suggest that inhibitors molecules are strongly adsorbed onto mild steel surface. The $\Delta G°_{ads}$ Values obtained for the inhibitors at studied temperature around –40 kJ mol^{-1} in acidic medium. These values indicate that the adsorption process of the evaluated inhibitors on the mild steel surface may involve chemisorptions.

Table 4: Thermodynamic parameters for the corrosion of mild steel in 1 M HCl in the absence and presence of different concentrations of P3 and P4.

Inhibitor	Linear correlation R	Slope	K (M^{-1})	$\Delta G°_{ads}$ (kJ.mol^{-1})
P3	0.99998	1.24541	1.9510^{05}	-41.45
P4	0.99993	1.14462	1.7510^{05}	-41.17

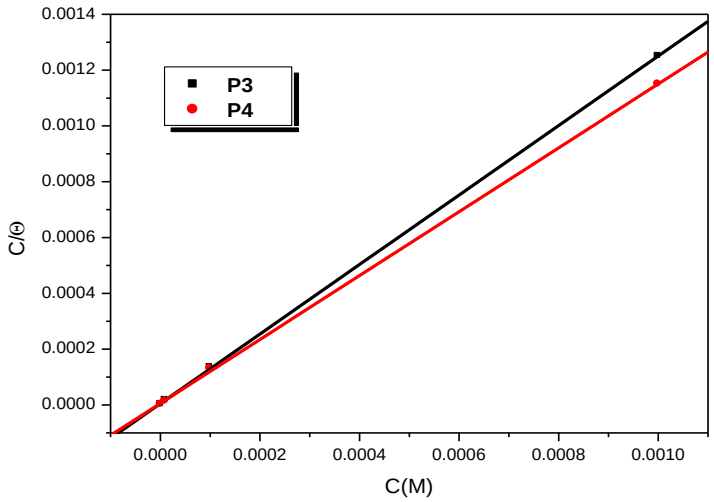

Figure 9: Langmuir adsorption isotherm of P3 and P4 on mild steel in 1M HCl at 308 K.

3.5. Computational theoretical studies

The FMOs (HOMO and LUMO) are very important for describing chemical reactivity. The HOMO containing electrons, represents the ability (E_{HOMO}) to donate an electron, whereas, LUMO haven't not electrons, as an electron acceptor represents the ability (E_{LUMO}) to obtain an electron. The energy gap between HOMO and LUMO determines the kinetic stability, chemical reactivity, optical polarizability and chemical hardness–softness of a compound [32]. In this study, the HOMO and LUMO orbital energies were calculated using B3LYP method with 6-31G which is implemented in Gaussian 09 package [33-34]. All other calculations were performed using the results with some assumptions. The higher values of E_{HOMO} indicate an increase for the electron donor and this means a better inhibitory activity with increasing adsorption of the inhibitor on the metal surface, whereas the lower values of E_{LUMO} indicates the ability to accept electron of the molecule. The adsorption ability of the inhibitor to the metal surface increases with increasing of E_{HOMO} and decreasing of E_{LUMO}. The HOMO and LUMO orbital energies of the **P3** and **P4** inhibitors were performed and were given and shown in (**Table 5**) and (**Figure 10**), respectively. High ionization energy (> 6 eV) indicates high stability of **P3** and **P4** inhibitors [35]. The number of electrons transferred (ΔN), dipole moment, ionization

potential**,** electron affinity, electronegativity, hardness, softness and total energy were also calculated and tabulated in (**Table 5**).

Table 5: Quantum chemical parameters for **P3** and **P4** obtained in gaseous and aqueous phases using the DFT at the B3LYP/6-31G level.

Parameter	Gaseous Phase		Aqueous Phase	
	P3	**P4**	**P3**	**P4**
Total Energy *TE* (eV)	-30138.5	-37462.0	-	-37454.1
E_{HOMO} (eV)	-6.5679	-6.3979	-6.6613	-6.7424
E_{LUMO} (eV)	-0.2359	-0.1902	-0.1785	-0.9572
Gap ΔE (eV)	6.3320	6.2077	6.4828	5.7851
Dipole moment μ (Debye)	2.9008	2.4373	3.9752	4.1360
Ionization potential I (eV)	6.5679	6.3979	6.6613	6.7424
Electron affinity A	0.2359	0.1902	0.1785	0.9572
Electronegativity χ	3.4019	3.2940	3.4199	3.8498
Hardness η	3.1660	3.1038	3.2414	2.8926
Electrophilicity index ω	1.8277	1.7479	1.8041	2.5619
Softness σ	0.3159	0.3222	0.3085	0.3457
Fractions of electron transferred ΔN	0.5682	0.5970	0.5522	0.5445

The nucleophilicity index (ω) is higher for the **P4** inhibitor than for **P3**, which indicates that **P4** is much richer of electrons than **P3**. The energy gap ΔE is larger for **P3** than for **P4** providing therefore a low reactivity of the **P3**.The E_{HOMO} in aqueous phase is higher in the **P4** than in the **P3**, an indication that benzyl group increases the electron donating capacity of the **P4** inhibitor.

The value of ΔN (number of electrons transferred) show that the inhibition efficiency resulting from electron donation agrees with Lukovit's study [36]. If $\Delta N < 3.6$, the inhibition efficiency increases by increasing electron donation ability of these inhibitors to donate electrons to the metal surface [37]. The value of ΔN of **P4** (0.5970 and 0.5445 in gaseous and aqueous phases, receptively) is lighter than **P3** (0.5682 and 0.5522 in gaseous and aqueous phases, respectively), this indicates that **P4** is more electron donor compared to **P3**.

(**Tables 6** and 7) display the most relevant values of the natural population (P(N), P(N-1) and P(N+1)) with the corresponding values of the Fukui functions (f_k^+, f_k^- and f_k^0) of the studied inhibitors. The calculated values of the f_k^+ for **P3** and **P4** inhibitors are mostly localized on the benzothiazine ring, namely C_1, C_2, O_{12}, and O_{14} (P3) and O_{12}, N_{13}, C_{15}, C_{19} and C_{28} (P4), indicating that the benzothiazine ring may be the most probable favorite site for nucleophilic attack.

Table 6. Pertinent natural populations and Fukui functions of **P3** calculated at B3LYP/6-31G in gaseous (G) and aqueous phases.

Atom k	***Phase***	***P(N)***	***P(N-1)***	***P(N-1)***	f_k^-	f_k^+	f_k^0
C_1	**G**	5,3116	6,2359	5,3105	0,9244	0,0011	0,4627
	A	5,2975	5,3987	5,2800	0,1012	0,0175	0,0593
C_2	**G**	5,857	5,9229	5,8097	0,0650	0,0481	0,0566
	A	5,8595	5,8888	5,7597	0,0293	0,0998	0,0645
O_{12}	**G**	8,6086	8,6983	8,5090	0,0897	0,0996	0,0946
	A	8,6415	8,7135	8,5422	0,0720	0,0994	0,0857
O_{14}	**G**	15,6943	15,8202	15,458	0,1259	0,2357	0,1808
	A	15,7084	16,3933	15,3849	0,6849	0,3235	0,5042

Table 7. Pertinent natural populations and Fukui functions of **P4** calculated at B3LYP/6-31G in gaseous (G) and aqueous phases.

Atom k	*Phase*	*P(N)*	*P(N-1)*	*P(N-1)*	f_k^-	f_k^+	f_k^0
O_{12}	**G**	8,6229	8,6876	8,5666	0,0647	8,6230	0,0605
	A	8,6135	8,7197	8,5916	0,1062	0,0220	0,0641
N_{13}	**G**	7,4384	7,4636	7,3879	0,0252	0,0505	0,0379
	A	7,4427	7,4512	7,3718	0,0085	0,0709	0,0397
C_{15}	**G**	6,2404	6,3640	6,2654	0,1236	-0,0249	0,0493
	A	6,2525	6,3181	6,2163	0,0656	0,0362	0,0509
C_{19}	**G**	6,1759	6,2991	6,1174	0,1232	0,0585	0,0908
	A	6,1293	6,3236	6,1123	0,1943	0,0170	0,1057
C_{28}	**G**	6,2221	6,3153	6,1491	0,0932	0,0730	0,0831
	A	6,2077	6,3143	6,1656	0,1065	0,0421	0,0743

The geometry of **P3** and **P4** in gaseous and aqueous phases (**Figure 10**) was fully optimized using DFT based on Beck's three parameters exchange functional and Lee–Yang–Parr nonlocal correlation functional (B3LYP)[38-40] and the 6–31G. The optimized molecular and selected angles, dihedral angles and bond lengths of **P3** and **P4** are given in (**Figure 10**). The optimized structure shows that the molecule P3 and have a non-planar structure. The HOMO and LUMO electrons density distributions of **P3** and **P4** are given in (**Table 8**).

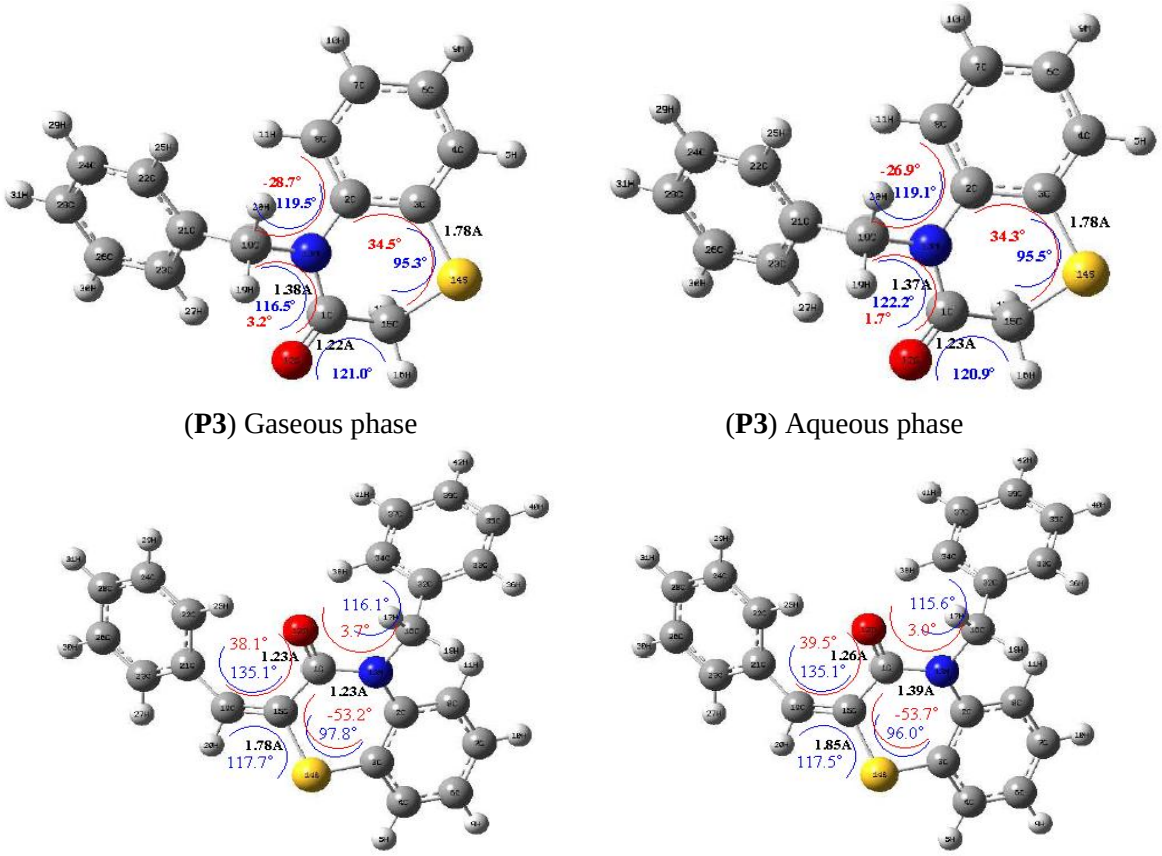

(**P3**) Gaseous phase (**P3**) Aqueous phase

(**P4**) Gaseous phase (**P4**) Aqueous phase

Figure 10: Optimized molecular structures and selected dihedral angles (red), angles (blue) and bond lengths (black) of the studied inhibitors calculated in gaseous and aqueous phases using the DFT at the B3LYP/6-31G level.

ISSN : 2028-2508
CODEN: JMESCN

Table 8: The HOMO and the LUMO electrons density distributions of **P3** and **P4** in gaseous and aqueous phases computed at B3LYP/6-31G level for neutral forms.

Inhibitor	Type of MO	Gaseous Phase	Aqueous Phase
P3	HOMO	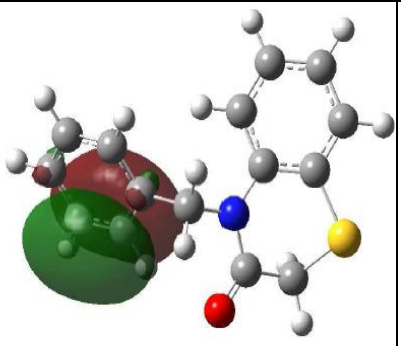	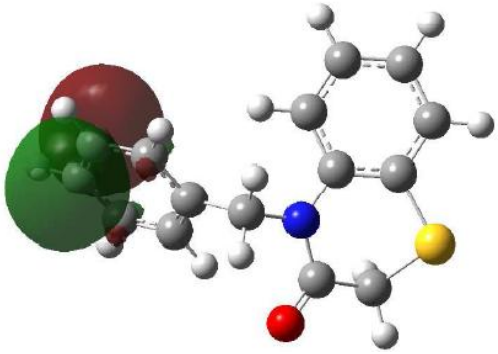
	LUMO	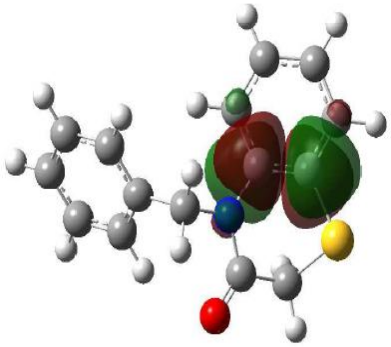	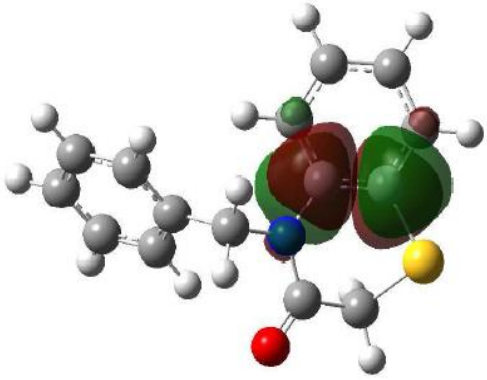
P4	HOMO	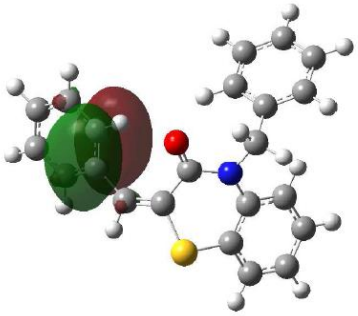	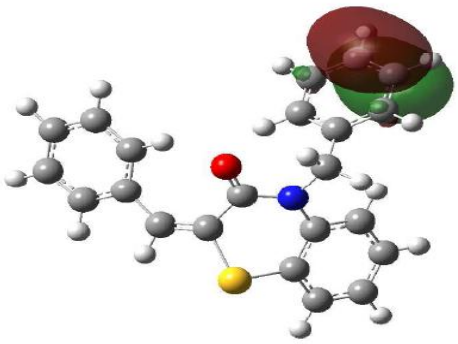
	LUMO	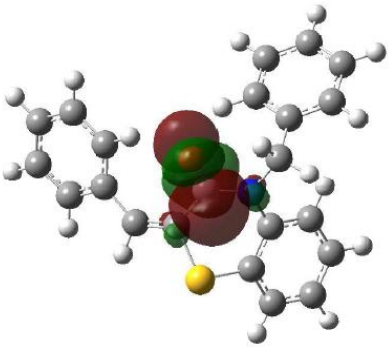	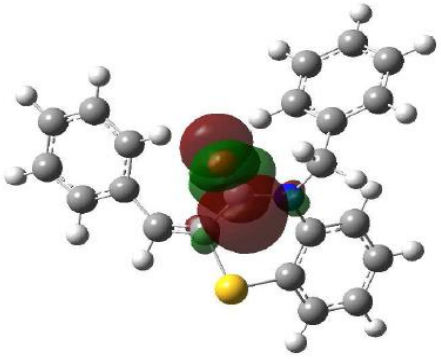

The large efficiency inhibition of **P4** with respect to **P3** is due to the presence of the benzyl group in **P4** inhibitor, which is electron-rich (π electrons), which increases the electron donor character of **P3.**

Conclusions

The following conclusions may be drawn from the study:

- P3 and P4 inhibit the corrosion of mild steel in 1M HCl. P4 is found to be more effective.
- The inhibition efficiency increases with increasing of inhibitor concentration to attain a maximum value of 95 % for inhibitor P4 at 10^{-3} M.
- Polarization study shows that 1,4-benzothiazine derivatives act as mixed-type inhibitors.
- Impedance method indicates that P4 adsorbs on the mild steel surface with increasing transfer resistance and decreasing of the double-layer capacitance.
- Inhibition is because of adsorption of the inhibitor molecules on the steel surface, thus blocking its active sites. Adsorption of the inhibitors fits a modified Langmuir isotherm model.
- Theoretical calculations (quantum chemical) are in good agreement with results obtained from electrochemical study and structure–corrosion protection relationships, which also confirm that the adsorption centre is S atoms.

Reference

1. Shaker M.A., Abdel-Rahman H.H., *Am. J. Appl. Sci*. 4(2007) 554.
2. Xia S., Qiu M., Yu L., Liu F., Zhao H., *Corros. Sci.* 50(2008) 2021.
3. El-Naggar M.M., *Corros. Sci*. 49(2007) 2226.
4. Gece G., *Corros. Sci*. 50(2008) 2981.
5. Awad M.K., Issa R.M., Atlam F.M., *Mater. Corros*. 60(2009) 813.
6. Behpour M., Ghoreishi S.M., Soltani N., Salavati-Niasari M., Hamadanian M., Gandomi A., *Corros Sci*. 50(2008) 2172.
7. Quraishi M.A., Sardar R., Jamal D., *Mater. Chem. Phys*. 71(2001**)** 309.
8. Park M. S., Chang E. S., Lee M. S., Kwon S. K., *Bull. Korean Chem. Soc.* 23(2002) 1836-1838.
9. Armenise D., Muraglia M., Florio M. A., De Laurentis N., Rosato A., Carrieri A., Corbo F., Franchini C., *Arch. Pharm.* 345(2012**)**407–416.
10. Sabatini S., Kaatz G. W., Rossolini G. M., Brandim D., Fravolini A., *J. Med. Chem*, 51(2008) 4321-4330.
11. Zia-ur-Rehman M., Choudary J. A., J.Elsegood M. R., Siddiqui H. L., Khan K. M., *Eur. J. Med. Chem. 44*(2009)1311-1316.
12. Vidal A., Madelmont J. C., Mounetou E., *Synthesis. 4(*2006)591-594.
13. Uhrhan P., Krauthausen E., *Eur. Patent EP*. 6108219 (1982).
14. Grigor'ev B. P., Gershanova I. M., Kravchenko B. M., *Zashch. Met. 28*(1992)833-836.
15. Pearson R.G., *Inorg. Chem*.27 (1988) 734-740.
16. Sastri V.S., Perumareddi J.R., *Corrosion*. 53 (1997) 617-622.
17. Elmsellem H., Nacer H., Halaimia F., Aouniti A., Lakehal I., Chetouani A., Al-Deyab S. S., Warad I., Touzani R., Hammouti B, *Int. J. Electrochem. Sci*. 9(2014)5328.
18. Elmsellem H., Basbas N., Chetouani A., Aouniti A., Radi S., Messali M., Hammouti B., *Portugaliae. Electrochimica. Acta*. 2(2014)77.
19. Udhayakala P., Rajendiran T. V., Gunasekaran S., *Chem. J.Biol. Phys. SCI.A.* 2(3) (2012)1151-1165.
20. Roy R.K., Pal S., Hirao K., *J. Chem. Phys*. 110(1999)8236.
21. Elmsellem H., Youssouf M. H., Aouniti A., Ben Hadd T., Chetouani A., Hammouti B., *Russian, Journal of Applied Chemistry*. 87(6) (2014) 744.
22. Elmsellem H., Harit T., AounitiA., Malek F., Riahi A., Chetouani A., Hammouti B., *Protection of Metals and Physical. Chemistry of Surfaces.* 51(5) (2015) 873.
23. Elmsellem H., Elyoussfi A., Sebbar N. K., Dafali A., Cherrak K., Steli H., Essassi E. M., Aouniti A. and Hammouti B., *Maghr. J. Pure & Appl. Sci*.1 (2015) 1-10.
24. Elmsellem H., Aouniti A.,Khoutoul M., Chetouani A., Hammouti B., Benchat N., Touzani R. and Elazzouzi M., *J. Chem. Pharm. Res*. 6 (2014) 1216.

25. Elmsellem H., AounitiA., Youssoufi M.H., BendahaH., Ben hadda T., Chetouani A., Warad I., Hammouti B., *Phys. Chem. News*. 70 (2013) 84.
26. Elmsellem H., Elyoussfi A., Steli H., Sebbar N. K., Essassi E. M., Dahmani M., El Ouadi Y., Aouniti A., El Mahi B., Hammouti B., *Der Pharma Chemica*. 8(1) (2016) 248.
27. Aouniti A., Elmsellem H., Tighadouini S., Elazzouzi M., Radi S., Chetouani A., Hammouti B., Zarrouk A., *Journal of Taibah University for Science*. (2015). http://dx.doi.org/10.1016/j.jtusci.2015.11.008.
28. Sebbar N. K., Elmsellem H., Boudalia M., lahmidi S., Belleaouchou A., Guenbour A., Essassi E. M., Steli H., Aouniti A., *J. Mater. Environ. Sci*. 6 (11)(2015)3034-3044.
29. Elmsellem H., Karrouchi K., Aouniti A., Hammouti B., Radi S., Taoufik J., Ansar M., Dahmani M., Steli H. and El Mahi B., *Der Pharma Chemica*. 7(10)(2015)237-245.
30. Chakib I., Elmsellem H., Sebbar N. K., Lahmidi S., Nadeem A., Essassi E. M., Ouzidan Y., Abdel-Rahman I., Bentiss F., Hammouti B., *J. Mater. Environ. Sci*. 7(6)(2016)1866-1881.
31. El Azzouzi M., Aouniti A., Tighadouin S., Elmsellem H., Radi S., Hammouti B., El Assyry A., Bentiss F., Zarrouk A. (2016).DOI: 10.1016/j.molliq.2016.06.007
32. Govindarajan M., Karabacak M., *Spectrochim.Acta Part A Mol Biomol.Spectrosc*. 85 (2012)251-60.
33. Becke A.D., *J. Chem. Phys*. 98 (1993) 1372.
34. Filali Baba Y., Elmsellem H., Kandri Rodi Y., Steli H., AD C., Ouzidan Y., Ouazzani Chahdi F., Sebbar N. K., Essassi E. M., Hammouti B., *Der Pharma.Chemica*. 8(4)(2016)159-169.
35. Hjouji M. Y., Djedid M., Elmsellem H., Kandri Rodi Y., Benalia M., Steli H., Ouzidan Y., Ouazzani Chahdi F., Essassi E. M., Hammouti B., *Der Pharma Chemica*. 8(4)(2016)85-95.
36. Lukovits I., Kalman E., Zucchi F., *Corrosion*. 57 (2001)3-7.
37.Sikine M., KandriRodi Y., Elmsellem H., Krim O., Steli H., Ouzidan Y., Kandri Rodi A., Ouazzani Chahdi F., Sebbar N. K., Essassi E. M., *J. Mater. Environ. Sci*. 7 (4) (2016) 1386-1395.
38. Elmsellem H., Elyoussfi A., Steli H., Sebbar N. K., Essassi E. M., Dahmani M., El Ouadi Y., Aouniti A., El Mahi B., Hammouti B., *Der. Pharma. Chemica*. 8(1) (2016) 248-256.
39. Lee C., Yang W., Parr R.G., *Phys. Rev. B.* 37 (1988) 785.
40. Hjouji M. Y., Djedid M., Elmsellem H., Kandri Rodi Y., Ouzidan Y., Ouazzani Chahdi F., Sebbar N. K., Essassi E. M., Abdel-Rahman I., Hammouti B., *J. Mater. Environ. Sci.*7(4) (2016) 1425-1435.